5

# Plasma Sprayed Bioceramic Coatings on Ti-Based Substrates: Methods for Investigation of Their Crystallographic Structures and Mechanical Properties

Ivanka Iordanova[1], Vladislav Antonov[2],
Christoph M. Sprecher[3], Hristo K. Skulev[4] and Boyko Gueorguiev[3]
[1]*University St. Kliment Ohridski, Sofia,*
[2]*Academy of Sciences, Sofia,*
[3]*AO Research Institute Davos, Davos,*
[4]*Technical University of Varna, Varna,*
[1,2,4]*Bulgaria*
[3]*Switzerland*

## 1. Introduction

Recently, life expectancy has been rising due to improvements in public health, nutrition, medicine and health-related quality-of-life requirements. However, aging leads to osteoporosis, i.e. loss of bone substance, associated with an increased risk of fracture. That is why in the field of orthopaedics and traumatology the number of patients receiving metal, and especially titanium-based, implants to correct skeletal defects and diseases is increasing worldwide. Critical factors for long-term stability of fixation include biocompatibility, material selection and implant design. Their investigation and optimisation, especially in case of implants coated with bioceramics, require further improvement of the existing and development of new methods for applied research in the structure and operational properties.

## 2. Ti-based implants with bioceramic coatings

Titanium (Ti) and some of its alloys, such as Ti-6Al-4V (TAV) and Ti-6Al-7Nb (TAN), are widely used for repair or replacement of parts of the human musculoskeletal system because of their biocompatibility, corrosion resistance in biological environments, low specific weight and excellent mechanical properties (Duan & Wang, 2006). However, when used in medical implants these biomaterials are exposed to bodily fluids under intensive mechanical loading. In such cases, it is necessary to meet the requirements for chemical and structural stability combined with reliable strength, wear resistance and good mechanical fixation. Despite high biocompatibility, long term observations show a certain amount of implant loosening, attributed to the lack of sufficient bioactivity of the surface over time (Suchanek & Yoshimura, 1998).

It has been found that covering the implant surface with bioceramic coatings, such as calcium orthophosphates or titania ($TiO_2$), can speed up the process of bone integration, thus enhancing the long-term fixation and implant stability (LeGeros, 2002; Suchanek & Yoshimura, 1998). Therefore, the bioceramic coatings and calcium orthophosphates in particular, applied on Ti-based substrates, having a useful combination of biocompatibility, mechanical properties and relative stability in bodily environment, are subjects of an increasing interest for biomedical applications in modern orthopaedics and dentistry (Gaona et al., 2007; Salman et al., 2008; Soares et al., 2008; Thomas, 1994).

Calcium orthophosphates are compounds of calcium (Ca) and phosphorous (P) in differing of calcium-phosphate ratios. Calcium hydroxylapatite (HA) $Ca_5(PO_4)_3(OH)$ is the most chemically stable and least soluble in aqueous media (Nelea et al., 2007). The composition and structure of the calcium hydroxylapatite are very similar to those of the bone mineral content that comprises about 70 % of the volume. This is the main reason for the observed high biointegration of HA coatings.

In contrast, $TiO_2$ and its deposits are generally considered as bioinert, i.e. not initiating a response or interaction in contact with biological tissues. However, it was recently indicated that the titania surface bioactivity can be activated by different chemical treatments (Gaona et al., 2007; Zhao et al., 2007). This could provoke reconsideration of the titania coatings role, making them superior to other biomedical coatings, as so far $TiO_2$ is mostly recognized with its excellent corrosion resistance and high adhesion strength to different substrates (Liu et al., 2006).

The in vivo performance of an implant, whose surface is covered with a bioceramic coating, enables a more stable fixation, due to better bonding to bone tissue, and decreased release of metal ions into the human body (Heimann, 2002; Yu-Peng et al., 2004). The goal of coating implants is to take advantage of mechanical strength, ductility, wear resistance and ease of fabrication of their metallic body in combination with good osteointegration and chemical stability associated with the applied surface layer (Chou & Chang, 2002).

## 3. Plasma-spraying of bioceramic coatings

Bioceramic coatings can be applied on Ti-based substrates by a number of methods, but undoubtedly plasma-spraying with its three environmental variations air plasma-spraying (APS), controlled atmosphere plasma-spraying (CAPS) and vacuum plasma-spraying (VPS) has proved to be one of the leading technologies in the medical practice for implant production.

Utilizing this technology, coatings are usually formed from powder particles, injected into a high temperature field, created in a plasma torch (plasmotron), where they are accelerated, molten and propelled towards the coated surface (Dhiman & Chandra, 2007; Gueorguiev et al., 2009b). The plasma gas (usually argon, nitrogen, or their mixture with hydrogen) is introduced into the plasma torch, where an electric arc transforms it to a plasma state with high enthalpy and temperature in the range 10000 - 30000°C (Brossa & Lang, 1992; Gill & Tucker, 1986). Although the injected powder particles are exposed to this high temperature for a very short time ($10^{-3} - 10^{-4}$s), most of them are sufficiently heated to become molten (Brossa & Lang, 1992). Reaching the coated surface, each particle solidifies independently in strongly non-equilibrium conditions and transforms into a disk-shaped solid splat (lamella)

(Brossa & Lang, 1992). However, the initial powder particles usually differ in shape, dimensions, temperature and velocity that can result in evaporation, partial melting or even absence of melting of some particles (Brossa & Lang, 1992; Nicoll et al., 1985). The evaporated particles do not take part in the coating formation. However, the partially molten and some completely unmolten particles could get incorporated in the coating, causing formation of inhomogeneous and porous structure. The partially molten particles solidify on the surface as spherical grains that can get depleted or become sources of internal stress fields in the coating, influencing substantially its properties and performance (Brossa & Lang, 1992; Iordanova et al., 2001).

Residual stresses, preferred crystallographic orientations (crystallographic textures) and pores are often observed in plasma-sprayed coatings (Gergov et al., 1990; Iordanova & Forcey, 1991). In some cases decomposition of HA during plasma-spraying is possible according to the following reaction:

$$Ca_5(PO_4)_3(OH) \rightarrow CaO + Ca_3P_2O_8 \text{ (or } CaO + Ca_4P_2O_9) \quad (1)$$

It has been found that the decomposition process is more pronounced when the HA powder particles are smaller and the spraying voltages are higher (Morris & Ochi, 1998).

The main advantages of plasma-spraying technology to coat Ti-based implants with bioceramic coatings are the high speed of coating deposition onto large surfaces, economy and high efficiency, combined with superior mechanical coating properties and chemical stability in a bodily environment enabling stable mechanical fixation (Gaona et al., 2007; Khor et al., 2004; McPherson et al., 1995; Morris & Ochi, 1998). The main disadvantage concerns the relatively poor adhesion between implant surface and applied deposit, observed in a number of cases. That is why, in order to prevent depletion, a transition layer is often plasma-sprayed prior to the main coating. For example, titania, being used as a single layer coating, can alternatively be plasma-sprayed as a transition layer between the top HA coating and the substrate, or as an incorporated reinforcing additive in composite coatings together with HA (Salman et al., 2008; Yu-Peng et al., 2004). Thus, in most of the cases, the adhesive and cohesive strength of the coating can be further increased and the interface strengthened (Chou & Chang, 2002; Yu-Peng et al., 2004). It is assumed that double-layer implant systems, consisting of a Ti-based body, a $TiO_2$ transition layer and an osteoconductive top HA coating will be able to withstand not only high local compression stresses, but also tensile and shear stresses, occurring during the micro-movements of the patient in the first stages of the healing phase after implantation (Heimann, 2002; Heimann et al., 2004). The presence of $TiO_2$ transition layer could also reduce the mismatch of the thermal expansion coefficients between the substrate and the top HA coating, which appears to be the main reason for failure at the interface between dissimilar materials (Salman et al., 2008).

Despite the positive results obtained using plasma-sprayed bioceramic coatings, there are still some concerns, especially regarding the durability and successful long-term performance of the implants (Cofino et al., 2004; Morris & Ochi, 1998; Sun et al., 2002). Moreover, in spite of its importance, the structure-formation process of plasma-sprayed bioceramic coatings has not been studied in detail so far. That is why it is necessary to investigate the structure formation of the deposits as a function of the technological conditions and their influence on the final implant operational properties. Furthermore, the mechanism for modification of HA coating

properties by deposition of $TiO_2$ transition layers or additives is not widely reported and the potential of plasma-sprayed titania coatings for bioactive applications has not been extensively explored yet (Salman et al., 2008; Yu-Peng et al., 2004).

The morphology and parameters of phase composition, interfaces, porosity, crystallographic textures, residual stresses, surface roughness, bond strength, availability of oxide inclusions and spherical grains are all critical parameters of the plasma-sprayed bioceramic coating structure, which must be considered, controlled and optimised. However, the knowledge about these parameters and their influence on the operational properties is still insufficient.

The application of advanced plasma-sprayed bioceramic coatings with superior properties in the contemporary medicine and dentistry requires a deep understanding of the structure formation processes, their dependence on the technological conditions and influence on the operational properties.

## 4. Relation between technological conditions, micro-structure formation and operational properties of bioceramic plasma-sprayed coatings for biomedical purposes

Due to the complexity of the plasma-spraying process, the technological conditions play a crucial role and can significantly influence the coating structure and practical performance (Azarmi et al., 2008; Frayssinet et al., 2006; Sampath et al., 2003).

The technological regime during plasma-spraying is mainly defined by the following parameters (Azarmi et al., 2008; Harsha et al., 2008; Sarikaya, 2005; Skulev et al., 2005):

- Heat power of the plasma jet;
- Type, pressure and flow rate of the plasma and transporting gas;
- Type, mean size and size distribution, flow rate and shape of the injected powder particles;
- Location, angle and type of powder injection into the plasma jet;
- Roughness, purity and temperature of the coated surface;
- Spraying-off distance between the spraying gun and substrate surface;
- Speed relation between the spraying gun and coated surface;
- Type of the ambient atmosphere in the plasmotron.

Not all of the parameters listed above are independent. That can complicate the selection and control of the technological conditions.

For instance, the type, pressure and flow rate of the plasma gas have an effect on the heat power of the plasma jet. The latter could be kept constant by a certain variation of the plasma gas pressure and flow rate.

The location, angle and type of the powder injection in order to ensure a complete melting of the initial particles could be pre-defined to a certain degree by the plasma jet heat power, powder type, particle size and plasma gas pressure.

The powder type, particles shape, mean size, size distribution and flow rate, together with the location and the type of powder injection determine the transporting gas flow rate.

The plasma jet heat power, spraying-off distance and relative speed between the spraying gun and substrate influence significantly the temperature of the coated surface.

The type and flow rates of the plasma and transporting gas have a significant effect on the ambient atmosphere.

A scheme, showing the interaction between the main technological parameters during plasma-spraying, is given in Figure 1.

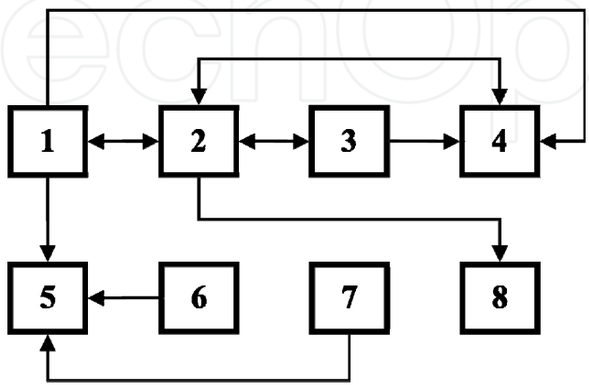


Fig. 1. Interaction scheme between the main parameters (1-8) determining the technological conditions during plasma-spraying: 1-heat power of the plasma jet; 2-type, pressure and flow rate of the plasma and transporting gas; 3-type, mean size and size distribution, flow rate and shape of the injected powder particles; 4-location, angle and type of powder injection into the plasma jet; 5-roughness, purity and temperature of the coated surface; 6-spraying-off distance between the spraying gun and substrate surface; 7-speed relation between the spraying gun and coated surface; 8-type of the ambient atmosphere in the plasmotron.

Initially the plasma-spraying processes and their influence on the coating properties have been investigated mainly empirically (Clyne & Gill, 1996). However, the contemporary requirements and high standards for operational properties of the bioceramic coatings lead to the necessity of a more complex approach to obtain fundamental knowledge about the structure formation processes and explore the dependence of their mechanisms and kinetics on the technological conditions. On the other hand, this complex approach is necessary to investigate the influence of coating composition and micro-structure parameters on their operational properties. This in turn has brought the necessity of more precise evaluation and control of the micro-structure parameters and technological conditions during plasma-spraying. As a result, further improvement of the existing and development of new experimental and theoretical methods and models for prognosis, investigation and control of the structure formation processes, technological parameters and operational properties has been provoked (Azarmi et al., 2008; Chen et al., 1993; Fan et al., 2005; Iordanova & Forcey, 1997; Kuroda & Clyne, 1991; Liu et al., 2005; Mawdsley et al., 2001; Moreau et al., 2005; Parizi et al., 2007; Sampath et al., 2003; Sarikaya, 2005; Toma et al., 2003). The main aim of this general trend for research and investigation, observed at present, is optimisation of the plasma-spraying technology to achieve superior parameters of the deposited bioceramic coatings enabling their successful and reliable long-term utilisation in a wide range of biomedical applications.

For this purpose, new techniques for visualisation and diagnostics of the injected powder particles during their flight to the coated surface have been developed (Moreau et al., 2005; Srinivasan et al., 2006; Streibl et al., 2006). New methods for non-destructive control, including statistical evaluation of the collected data, together with prognosis of the coating parameters as a function of the technological conditions have been offered as well (Zhu & Ding, 2000). Some work has already been done to characterise the following main dependencies that play an important role for successful performance of the discussed biomedical coatings (Azarmi et al., 2008; Boulos et al., 1993; Celik et al., 1999; Chen et al., 1993; Choi et al., 1998; Dyshlovenko et al., 2005; Fan et al., 2005; Gueorguiev et al., 2008a, 2008c; Iordanova & Forcey, 1997; Keller et al., 2003; Khor et al., 2004; Kreye et al., 2007; Kuroda & Clyne, 1991; Leigh & Berndt, 1997; Li & Khor, 2002; Liu et al., 2005; Lugscheiber et al., 1993; Mawdsley et al., 2001; Montavon et al., 1997; Moreau et al., 2005; Neufuss et al., 2001; Ohmori & Li, 1991; Parizi et al., 2007; Sampath et al., 2003; Sarikaya, 2005; Srinivasan et al., 2006; Staia et al., 2001; Streibl et al., 2006; Toma et al., 2003; Tong et al., 1996; Wallace & Ilavsky, 1998; Zhu & Ding, 2000):

- Relation between technological parameters, thermal and kinetic energy of the powder particles, their trajectories and stage of melting;
- Influence of the chemical composition and size of the powder particles and substrate parameters (composition, roughness, purity, temperature) on the morphology, phase composition, residual stresses and crystallographic texture of the applied coatings;
- Influence of the parameters, discussed above, on such important operational properties of the coatings as density, hardness, toughness, frictional characteristics, wear resistance, elasticity, thermal conductivity, structural and chemical stability.

Despite the lot of work that has been done so far, a generalised model allowing planning of technological conditions for production of coatings with pre-defined properties has not been developed yet. This is mainly due to the complexity of the plasma-spraying and structure formation processes. Their characterisation and understanding require development of new methods for further fundamental and applicable interdisciplinary analyses by involvement of highly qualified specialists from different fields.

## 5. Methods for analysis of crystallographic structures and mechanical properties of plasma-sprayed bioceramic coatings

The main methods applied and the latest results obtained by the authors of this chapter during the investigation of initial powders and plasma-sprayed hydroxylapatite and titania bioceramic coatings are discussed below.

### 5.1 Optical metallography and scanning electron microscopy

Optical metallography and scanning electron microscopy (SEM) have been applied to evaluate particle shape and size distribution parameters of initially injected powders as well as to analyse coating morphology, spherical grains, chemical composition and distribution of elements in bioceramic plasma-sprayed coatings.

#### 5.1.1 Particle shape and size distribution parameters of the initial powders

Mean size and size distribution of the initial powder particles are important parameters influencing the morphology and the macro-properties of the plasma-sprayed coatings.

Images, taken with transmission optical microscope of the initial bioceramic powders XPT-D-703 (HA) and AMDRY-6505 ($TiO_2$), produced by Sulzer Metco Europe GmbH (Switzerland), are shown in Figure 2.

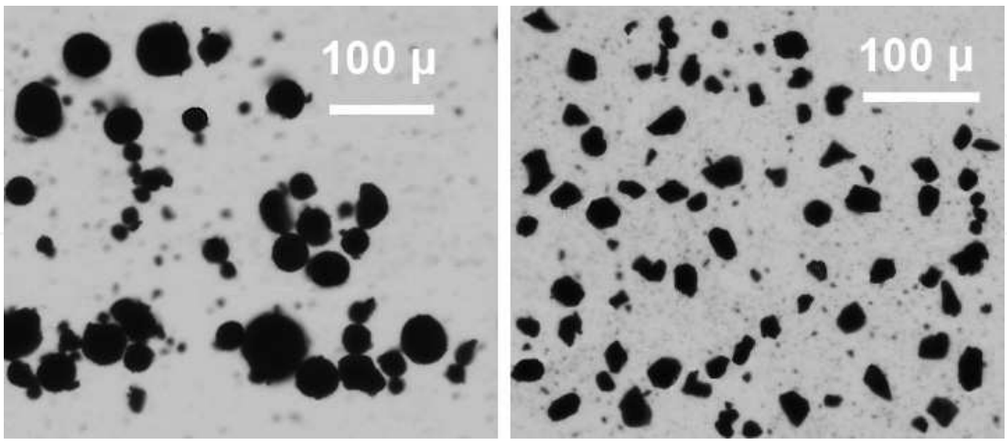


Fig. 2. Particles of powders XPT-D-703 (HA, left) and AMDRY-6505 ($TiO_2$, right), observed in transmission optical microscope (Gueorguiev et al., 2008a, 2008b).

It is obvious that the majority of the HA particles are spherical in contrast to the sharp-edged $TiO_2$ ones. Whereas the size of spherical particles is characterised with the diameter, the more asymmetric particle size has been evaluated via the following two parameters (Gueorguiev et al., 2008a, 2008b; Iordanova et al., 2001):

- Mean value between the measured maximum and minimum particle size;
- Average diameter $d_{opt}$ which is a function of the area $s_{opt}$ of the particle projection, evaluated with image analysis software (for example, Carl Zeiss AxioVision). The following equation is in power:

$$d_{opt} = 2\sqrt{s_{opt} / \pi} \tag{2}$$

Particle size distribution curves, based on several hundred measurements of randomly chosen particles, can be plotted and fitted with the following type of Gaussian function:

$$f = A \exp\left[-(x-c)^2 / b^2\right] \tag{3}$$

Characteristics of powder particle dimensions of the initial powders XPT-D-703 and AMDRY-6505, used for deposition of bioceramic plasma-sprayed coatings, are given in Table 1.

| Initial powder | Particle size ($d_{opt}$), µm | | |
|---|---|---|---|
| | Minimal | Maximal | Mean |
| XPT-D-703 (HA) | 3.76 | 89.15 | 39.70±11.35 |
| AMDRY-6505 ($TiO_2$) | 5.65 | 33.52 | 18.0±5.15 |

Table 1. Particle size parameters of two initial powders for plasma-spraying (Gueorguiev et al., 2008b).

### 5.1.2 Coating morphology, chemical composition and distribution of elements

Plasma-sprayed bioceramic coatings have been investigated at a cryo-fractured cross-section using scanning electron microscope (Hitachi S-4100 FESEM) equipped with a secondary electron (SE) detector for topographical imaging, a back scattered electron (BSE) one for density imaging and an energy dispersive X-ray (EDX) detector to analyse chemical composition (Burgess et al., 1999; Gueorguiev et al., 2009b; Iordanova et al., 1994, 1995). EDX has been applied for analysis of interfaces in double-layer plasma-sprayed bioceramic coatings, shown in Figure 3, together with the distribution of the main elements Ca, P and Ti at the interface between the transition $TiO_2$ and top HA layers.

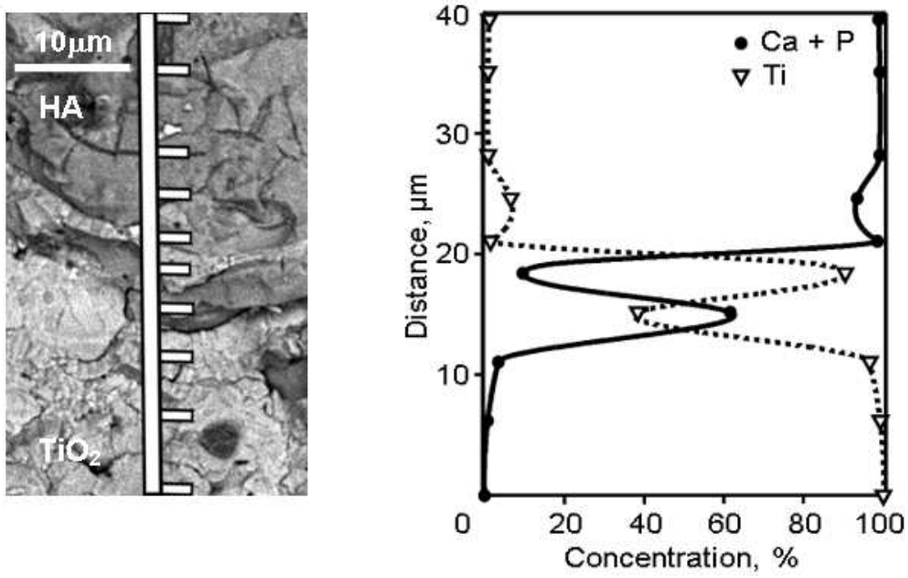


Fig. 3. SEM image (BSE mode) of the interface between the transition $TiO_2$ and top HA layers of a plasma-sprayed bioceramic coating (left) together with the corresponding EDX profile of Ca, P and Ti concentrations (right) (Gueorguiev et al., 2009b).

The observed element distribution shows that a diffusion zone, around 15 μm wide, with non-smooth change of the element concentration has been formed at the $TiO_2$-HA interface.

### 5.1.3 Stereological metallographic analysis of spherical grains

If during plasma-spraying the injected powder particles reach the coated surface in a partially molten state they can form grains with a spherical shape in the coating. The latter, being inhomogeneous inclusions in the matrix with a predominantly lamellar structure, can significantly influence the macro-properties and practical performance of the bioceramic coatings. For that reason the parameters of such spherical grains have to be analysed and controlled. Stereological metallographic methods developed for characterisation of plasma-sprayed and in particular bioceramic coatings are an excellent tool for this analysis (Gueorguiev et al., 2008b; Iordanova et al., 2001). Principally, these methods allow estimation of volume parameters of microstructure elements, based on their two-dimensional cross-section plane parameters that can be experimentally measured applying standard metallographic methods performed via optical or scanning electron microscopy.

All quantitative stereological analyses are based on the principle that the share of a phase (or any other structure element) in a volume is equal to the surface or linear share of its cross-sections with a plane or a line intersecting this volume, respectively. Only structure elements that can be represented as convex bodies are suitable for stereological analyses, as a concave ones can be crossed more than once by the intersecting plane or line. In addition, stereological methods are applicable when the distribution of the analyzed structure element in the volume is close to random.

A method, based on the Scheil-Schwartz-Saltikow technique, was developed by the authors of this chapter to evaluate volume parameters of spherical grains of interest in bioceramic coatings (Gueorguiev et al., 2008b). The analysis on double-layer coatings showed that the share of spherical grains in the top HA and in the transition $TiO_2$ layer was less than 1% and about 1.5% of the layer's volume, respectively.

### 5.2 Phase composition and crystallographic parameters characterised with X-ray powder diffraction

X-ray powder diffraction (XRD) experiments are performed in two configurations, namely symmetric Bragg-Brentano (B-B) and Grazing Incidence Asymmetric Bragg Diffraction (GIABD) modes (Gueorguiev et al., 2008c). Their schematics are represented in Figure 4.

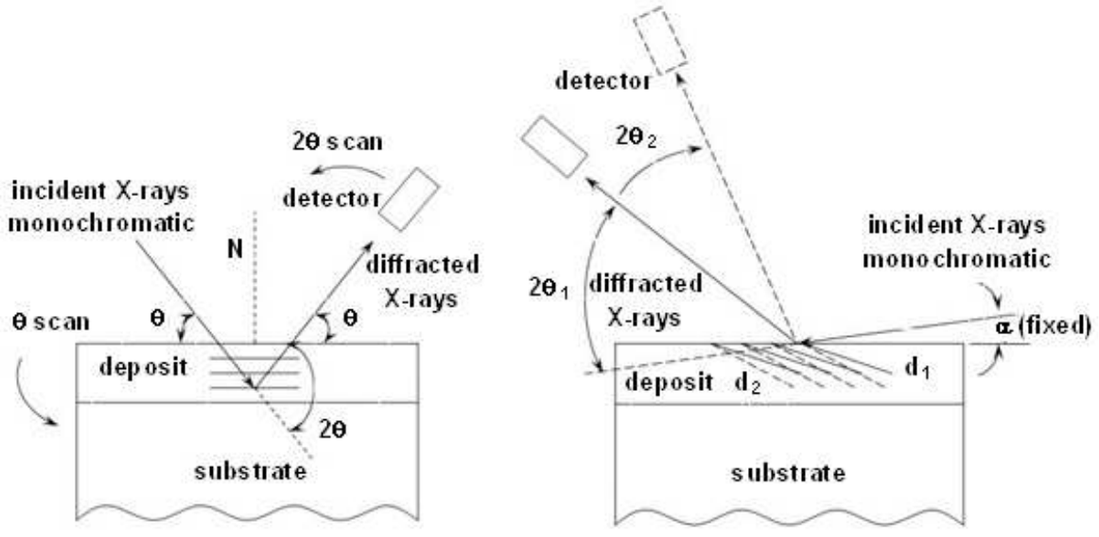


Fig. 4. Schematics of X-ray diffraction pattern registration in Bragg-Brentano (B-B, left) and Grazing Incidence Asymmetric Bragg Diffraction (GIABD, right) modes.

The registration in B-B mode is realized via standard synchronized θ-2θ scans of the sample and detector, where θ is the Bragg angle, and the registered patterns are resultant from crystallographic planes that are parallel to the surface (Figure 4, left).

In GIABD mode the sample is fixed in respect to the incident beam at a preset angle (α) and only the detector performs 2θ scans (Figure 4, right). Thus, the diffraction pattern is resultant from the interaction of the incident beam with the crystallographic planes in Bragg orientation, that are declined to the investigated surface at an angle ψ = θ - α (Iordanova et

al., 2002). In order to increase the ratio between the peak intensities and the background, a plane monochromator is usually used on the diffracted beam.

In both B-B and GIABD modes the XRD patterns have been registered stepwise with step size and counting times dependent on the parameter analyzed. The diffraction peaks have been background corrected and then least square fitted for estimation of their angular position (i.e. the peak centroid 2θ), intensity and broadening. Three analytical functions, namely Gaussian, Lorentzian or Pseudo-Voight have been used for this purpose. The analysed crystallographic parameters are described below.

### 5.2.1 Phase composition

In order to characterize the phase composition of the initial powders or plasma-sprayed ceramic coatings, XRD patterns have been registered in B-B mode with a relatively large angular interval (for example, 2θ between 15° and 105°) using Cu Kα characteristic radiation. Typical XRD patterns are presented in Figure 5.

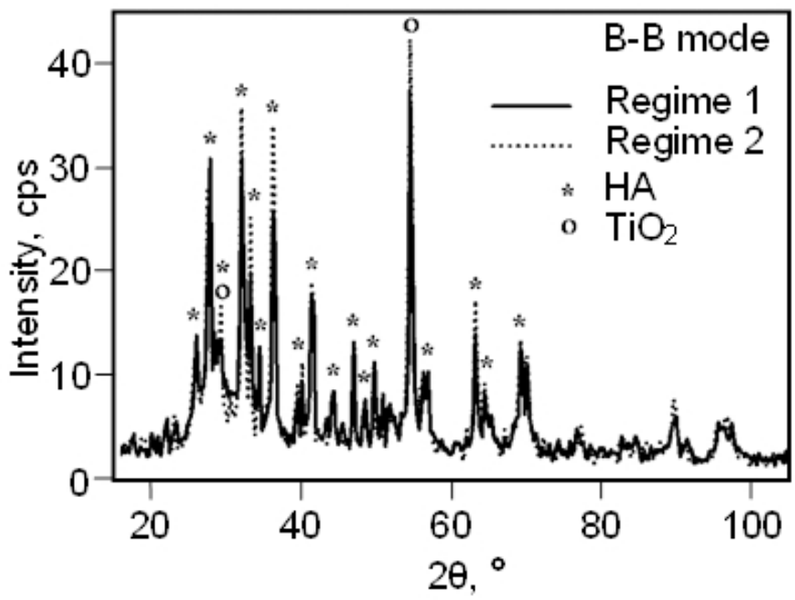


Fig. 5. XRD patterns registered in B-B mode from two double-layer bioceramic coatings with transition $TiO_2$ and top HA layers, deposited on TAV substrates in two different plasma-spraying regimes (Gueorguiev et al., 2008c).

The patterns are typical for materials with polycrystalline structure containing a number of diffraction peaks. However, the slightly increased hallo-like background within the angular interval 2θ between 23° and 35° points to the availability of a negligible amount of amorphous phase.

The qualitative phase analysis based on comparison between the angular positions 2θ of the registered diffraction peaks and the respective standard ASTM (JCPDS) values showed that the top and the transition layers correspond to crystalline HA with hexagonal unit cell, space group 176, $P6_3/m$ and β-$TiO_2$ with monoclinic symmetry, respectively (Gueorguiev et

al., 2008c, 2009b). Similar patterns have been registered for the respective initial powders as well. The comparison between the XRD patterns of the analyzed layers and the respective injected powders showed a qualitative coincidence, suggesting no decomposition of the initial powders during the plasma-spraying in both regimes.

### 5.2.2 Line broadening analysis

Broadening of diffraction peaks is analyzed via their full width at half maximum (FWHM). In general, this parameter is a function of lattice imperfections and non-homogeneous elastic deformation in the investigated material. Concerning plasma-sprayed coatings it has been found that in most cases the FWHM is higher for thinner coatings and coatings, deposited at lower substrate temperature, compared to thicker coatings and coatings on substrates, preheated to higher temperature. In our analyses a decrease of the FWHM during the growth of plasma-sprayed HA coatings was observed, which is considered to result from the steadily increasing substrate temperature during plasma-spraying.

Basic parameter related to the crystallographic structure perfection is the physical broadening $\beta_t$ that can be evaluated from the experimental FWHM. According to the Williamson-Hall model (Hemmati et al., 2006; Herrmann et al., 2002) the physical broadening of the XRD peaks is related to the crystallographic parameters of the investigated material according to equations (4) and (5) for Lorentzian and Gaussian fitting functions of the peak, respectively.

$$\beta_t = \frac{K\lambda}{D\cos\theta} + 2\varepsilon\tan\theta + \beta_0 \tag{4}$$

$$\beta_t = \sqrt{\left(\frac{K\lambda}{D\cos\theta}\right)^2 + (2\varepsilon\tan\theta)^2 + \beta_0^2} \tag{5}$$

K is the Sherrer constant, D is the dimension of the regions of coherent X-ray scattering, related to the crystalline size, ε is the lattice residual elastic micro-deformation, resultant from the available crystallographic defects and $\beta_0$ is an instrumental factor, influencing the line broadening.

### 5.2.3 Crystallographic texture analysis

It is well known that in plasma-sprayed coatings, being deposited in non-equilibrium conditions, crystallographic texture with axial symmetry, same as that of the spraying process, could be formed. According to the theoretical model, suggested by Iordanova and Forcey (Iordanova & Forcey, 1991; Gueorguiev et al., 2008a), if the energetic potential during plasma-spraying and the temperature at the substrate surface are relatively low, the axial (fiber, out-of-plane) texture is usually characterized with a preferable orientation of the most densely packed crystallographic planes of the coating crystallites parallel to the substrate surface.

Fiber crystallographic textures can be qualitatively characterized with one-dimensional orientation distribution functions (1D ODFs). For this purpose, a particular diffraction peak of the bioceramic coating with Bragg angle θ is registered in GIABD mode at several preset incident angles (α). Analogous registrations are performed for the same peak of a random

sample without texture (for example, powder of the same material fixed with special glue in the sample holder). Then the intensities of the coating peak at different incident angles are normalized to the corresponding intensities of the peak, registered for the random standard. The plotted normalised intensities versus angle ψ (where ψ=θ-α) represent the 1D ODF that provides a qualitative information about the formed fiber texture.

The availability of preferred crystallographic orientation in plasma-sprayed films and coatings can be characterized quantitatively with pole density $P_{\{hkl\}}$, which is proportional to the probability that a particular family of crystallographic planes {hkl} is parallel to the sample surface. The pole density can be calculated according to the following equation:

$$P_{\{hkl\}} = \frac{I^{film}_{\{hkl\}} / I^{st}_{\{hkl\}}}{(1/n)\sum(I^{film}_{\{hkl\}} / I^{st}_{\{hkl\}})} \quad (6)$$

where $I^{film}_{\{hkl\}}$ and $I^{st}_{\{hkl\}}$ are the intensities of the {hkl} diffraction peaks registered in B-B mode for the analyzed deposits and the texture-less powder standard, respectively, and n is the number of the analyzed peaks (only the lowest diffraction orders are considered).

Two histograms representing the relative shares of the HA crystallites, oriented with their {hkl} crystallographic planes parallel to the coating surfaces, are presented in Figure 6. The two analysed coatings differ by the thickness of the top HA layer (thin - 20μm, thick - 40 μm). It can be concluded that in none of these HA coatings a pronounced crystallographic texture has been formed.

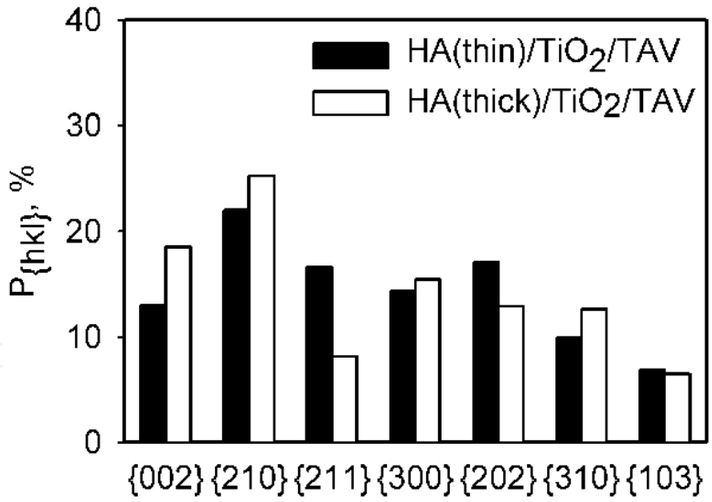


Fig. 6. Pole density histograms, representing the share of HA crystallites, oriented with their {hkl} planes parallel to the substrate surface in two double-layer plasma-sprayed coatings (thin and thick) with transition $TiO_2$ and top HA layers (Gueorguiev et al., 2009b).

### 5.2.4 Lattice parameters

Lattice unit-cell parameters of crystalline materials are among their most important crystallographic characteristics. They can give additional information about the phase composition and crystallographic perfection of the available phases. Lattice parameters can

be evaluated from the XRD patterns via the interplanar distances $d_{\{hkl\}}$ according to the equation based on the Bragg law:

$$d_{\{hkl\}} = \lambda / 2\sin\theta_{\{hkl\}} \tag{7}$$

where $\lambda$ is the wavelength of the used characteristic radiation and $\theta_{\{hkl\}}$ is the experimentally defined centroid of the {hkl} XRD peak.

Evaluation of lattice parameters for crystallites belonging to the {hkl} texture component requires registration of the corresponding {hkl} diffraction peak in B-B mode. Such an approach has been applied for calculation of the lattice parameter (c) for two plasma-sprayed HA coatings with hexagonal unit cell as follows (Gueorguiev et al., 2008c). Firstly, the interplanar $d_{\{002\}}$ distance has been evaluated from the {002} diffraction peak of the HA coating, registered in B-B mode as described above. Then the following relation, valid for the hexagonal HA lattice, has been used:

$$\frac{1}{d^2} = \frac{4}{3}\frac{(h^2 + hk + k^2)}{a^2} + \frac{l^2}{c^2} \tag{8}$$

For {002} diffraction peaks it transforms to:

$$\frac{1}{d_{002}^2} = \frac{4}{c_{002}^2} \tag{9}$$

Finally, the $c_{\{002\}}$ parameter has been evaluated via the relation:

$$c_{\{002\}} = 2d_{\{002\}} \tag{10}$$

The evaluated lattice parameters $c_{\{002\}}$ for the plasma-sprayed HA coatings are presented in Figure 7 together with the standard ASTM value. It is obvious that the experimental parameters are higher than the standard due to fixed compressive residual macro-stresses, acting parallel to the HA coating surface (Gueorguiev et al., 2008c).

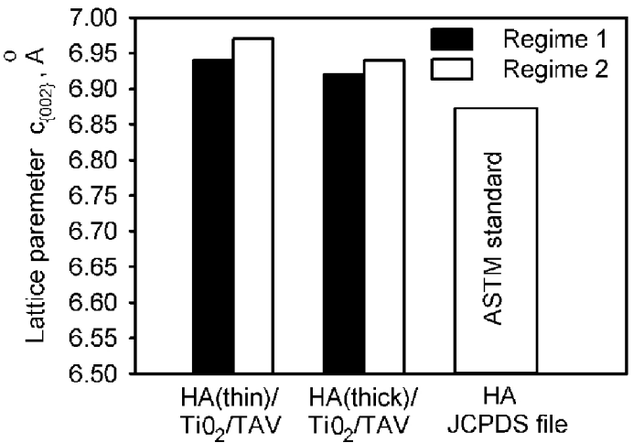


Fig. 7. Lattice parameters $c_{\{002\}}$ for the HA layer in two double-layer plasma-sprayed coatings with transition $TiO_2$ and top HA layers, differing in spraying regime and thickness, together with the respective standard JCPDS value (Gueorguiev et al., 2008c).

### 5.2.5 Residual macro-stresses

Residual macro-stresses are an important parameter of bioceramic coatings creating irreversible elastic deformation of the crystal lattice and significantly affecting properties and coating performance. Their evaluation via XRD methods is most often based on the Poisson's model, according to which the fixed residual stresses cause different elastic deformations in crystallites having different crystallographic orientations. The deformations can be evaluated via change of interplanar spacing in respect to the one existing prior to formation of residual stresses. The most suitable method for evaluation is called 'sin²ψ' (Prevey, 1986), where a chosen {hkl} peak has to be firstly registered in GIABD mode at different incident angles (α), followed by evaluation of the interplanar spacings $d_{\{hkl\}}$. Then the dependence $d_{\{hkl\}}$ versus $\sin^2\psi$ , where ψ=θ-α needs to be plotted and fitted linearly as shown in Figure 8.

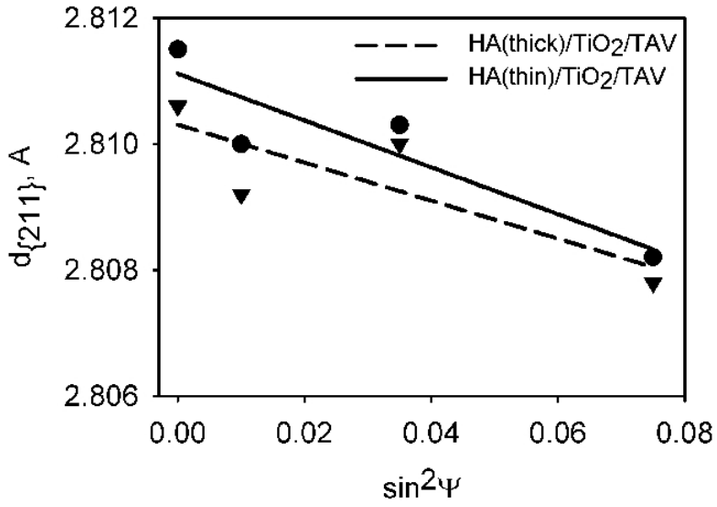


Fig. 8. Experimental data and least square linear fits of the dependencies of the interplanar HA spacing $d_{\{211\}}$ versus $\sin^2\psi$ for two double-layer plasma sprayed coatings with transition $TiO_2$ and top HA layers differing in thickness (Gueorguiev et al., 2009b).

According to the plane stress-strain model (Prevey, 1986) the values of the residual macro-stresses, acting parallel to the surface can be evaluated from the following equation (Prevey, 1986; Clyne & Gill, 1996):

$$\sigma = \frac{E}{1+\nu} \cdot \frac{1}{d_0} \cdot \left( \frac{\partial d_\psi}{\partial \sin^2 \psi} \right) \tag{11}$$

where E and ν are the Young's modulus and Poisson's ratio of the analysed material (HA in this particular case); $d_0$ and $\partial d_\psi / \partial \sin^2\psi$ are respectively the experimentally obtained y-intercept and gradient of the linear plots of the dependence $d_{\{hkl\}}$ versus $\sin^2\psi$.

As the XRD methods are based on diffraction and Young's modulus and Poisson's ratio are anisotropic parameters, also called X-ray elastic parameters as well, it is necessary to know their values in the crystallographic direction of the estimated interplanar distance. In addition, if E and ν have not been experimentally evaluated for the particularly investigated

material, they would need some corrections. For example, it is known that air plasma-sprayed coatings usually contain between 15 and 30 volume percent pores that are expected to decrease the E/v ratio about five times in respect that one obtained for monocrystals or bulk materials with the same composition (Kuroda & Clyne, 1991).

According to equation (11) for residual stress evaluation, the negative gradients observed in both fitted linear plots in Figure 8 indicate existence of compressive (negative) residual macro-stresses, acting parallel to the surface. Contrary to that, positive gradients indicate tensile (positive) residual stresses.

According to the model suggested by Kuroda and Clyne (Kuroda & Clyne, 1991), main components of fixed macro-stresses in plasma-sprayed coatings are quenching and thermal stresses. They can be quantitatively estimated from the equations offered by the same authors. However, some additional factors, such as possible plastic deformation, polymorphous phase transformations, relaxation processes (for example, cracking and bending), that could accompany the coating formation, must also be considered.

### 5.3 Porosity characterization

Due to micro-pores contained in the initial powder material or incomplete bonding between the lamellae in plasma-sprayed bioceramic coatings, a certain degree of porosity exists (Li & Ohmori, 2002; Li et al., 2004).

The relative porosity p is defined as follows [84]:

$$p[\%] = \left(1 - \frac{\rho_1}{\rho_0}\right) \cdot 100 \tag{12}$$

where $\rho_1$ and $\rho_0$ are coating and initial powder material densities, respectively (Tsui et al., 1998).

A suitable and relatively simple method for porosity estimation is a hydrostatic weighing method, involving measurements of the weight in air and in a liquid with known density (usually distilled water) (Gergov et al., 1990; Iordanova et al., 1995). For analysis of a plasma-sprayed coating, it is firstly necessary to separate a part of it from the substrate. Prior to immersing in the liquid, the analysed sample needs to be covered with vaseline in order to isolate its surface pores from the liquid. Then the porosity can be evaluated according to the following formula:

$$p[\%] = \left(1 - \frac{\frac{W_z \cdot \rho_w}{\rho_z}}{W - W' - \frac{W_v \cdot \rho_w}{\rho_v}}\right) \cdot 100 \tag{13}$$

where $W_z$ is the weight of the coating in air, $\rho_z$ is the density of the initial powder, W is the weight of the coating with vaseline and the elastic thread from which it is hung during weighing, W' is the weight of the sample on the thread immersed in water, $W_v$ is the weight of the applied vaseline film, $\rho_v$ is the density of vaseline (handbook value usually taken as 0.88 g/cm$^3$) and $\rho_w$ is the distilled water density.

The density of the initial powder $\rho_z$ can be estimated by subsequent weighing in air and in distilled water from the following relation:

$$\rho_z = \frac{G_3 - G_2}{V_k - \frac{G_4 - G_3}{\rho_w}} \tag{14}$$

where $G_3$ is the weight of powder with the test tube, $G_2$ is the weight of the empty test tube, $V_k$ is the volume of the powder and water in the test tube, $G_4$ is the weight of the test tube with powder and distilled water, and $\rho_w$ is the distilled water density.

The porosity of plasma-sprayed ceramic coatings for medical needs must be controlled to be relatively low in order to achieve better adhesion, suitable mechanical properties and lower brittleness of the deposits. On the other hand, higher porosity is expected to enhance bone ingrowth during the healing process in the human body.

### 5.4 Tensile bond strength between substrate and plasma-sprayed coating

Adhesion (tensile bond strength) between substrate and plasma-sprayed coating is usually measured via pull-out mechanical tests according to ASTM C633-79 (Ding et al., 2001; Gueorguiev et al., 2008c). For this purpose, prior to testing the coated surface is glued to a grit-blasted stainless-steel cylindrical counter body with special adhesives (for example, HTK Ultra Bond, Hanseatisches Technologie Kontor GmbH). Then a tensile force is applied to deplete the counter body. A schematic of a pull-out test, together with a picture of a test setup, are shown in Figure 9.

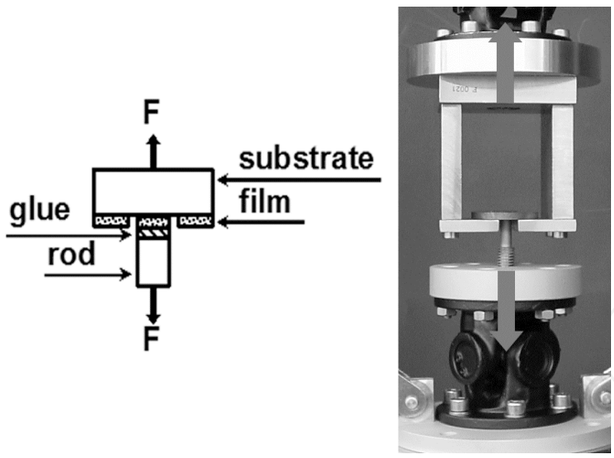


Fig. 9. Schematic of a pull-out test (left) and example picture of a test setup (right) (Gueorguiev et al., 2008c).

Several coatings of each kind are usually tested and the average of the maximum applied tensile mechanical stress γ, calculated according to the formula below, is defined as tensile bond strength of the deposit:

$$\gamma = \frac{F_{\max}}{S} \tag{15}$$

where $F_{max}$ is the depletion force and S is the area of the glued cylindrical counter body.

In general, similar tests can be applied for evaluation of the cohesion between different layers in multi-layer coatings.

### 5.5 Numerical methods for investigation of structural and mechanical parameters based on the density functional theory (DFT)

In order to estimate precisely residual stresses in HA bioceramic deposits, their Young's modules $E_{<uvw>}$ and Poisson's ratios $v_{<uvw>}$ in different crystallographic directions <uvw> have to be evaluated. A suitable way way can be the development of a numerical method, based on the density functional theory (DFT). This is a quantum mechanical theory to investigate electronic structure of many-body systems and condensed phases, where the electronic structure can be determined using functionals, i.e. functions of another function, the latter being in this case the electron density distribution. DFT is one of the most reliable and prospective methods for evaluation of structure and elastic properties of such systems. The calculations can be performed using appropriate software packages (for example, Quantum Espresso program code) to simulate the unit cell and estimate the values of the elastic constant matrix $C_{ij}$ and elastic compliance matrix $s_{ij}$ of the respective monocrystals (Giannozzi et al., 2009).

Then the $E_{<uvw>}$ and $v_{<uvw>}$ values can be calculated by means of pseudo-potentials and known crystallophysics relationships. The main algorithms are published in (Gonze, 1996; Monkhorst & Pack, 1976; Schlegel, 1982). Verification of the results is performed by comparison of the simulated unit cell parameters to those obtained from respective standard ASTM files. In a previous paper (Gueorguiev et al., 2009a) DFT was applied to simulate the crystallographic structure and estimate elastic constant and elastic compliance matrixes of HA monocrystal with hexagonal symmetry. The obtained HA unit cell is shown in Figure 10. Its symmetry, corresponding to $P6_3/m$ (space group 176) together with the values of the parameters a=9.418 Å and c=6.875 Å are in very good agreement with those from the standard ASTM file JCPDS 34-0010 for $P6_3/m$ HA (space group 176), which is a proof of correctly performed numerical simulations.

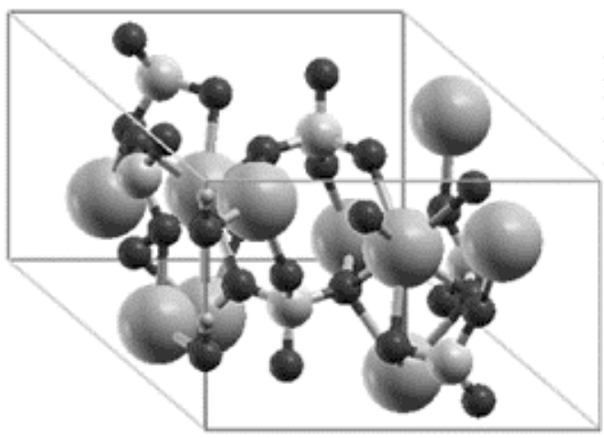

Fig. 10. DFT simulated unit cell of HA, space group 176, $P6_3/m$, with Ca, O, P and H atoms presented with big gray, black, middle-sized gray and small gray balls, respectively.

The values of the Young's modulus $E_{<uvw>}$ and Poisson's ratio $\nu_{<uvw>}$ have been derived from the values of the elastic constant matrix $C_{ij}$ and elastic compliance matrix $s_{ij}$ and the parameters of the unit cell a and c via the following relations (Sirotin & Shaskolskaya, 1983):

$$E_{<hkl>}^{-1} = \frac{\left\{\left(h^2+k^2-hk\right)^2 a^4 s_{11} + l^4 c^4 s_{33} + \left(h^2+k^2-hk\right) l^2 a^2 c^2 \left(s_{44}+2s_{13}\right)\right\}}{\left[\left(h^2+k^2-hk\right)a^2 + l^2 c^2\right]^2} + \frac{a^3 c\left[3\sqrt{3}hkl\left(h-k\right)s_{14} + l(2h-k)\left(2k^2-h^2+hk\right)s_{25}\right]}{\left[\left(h^2+k^2-hk\right)a^2 + l^2 c^2\right]^2} \tag{16}$$

$$\nu_{<hkl>} = \frac{3B - E_{<hkl>}}{6B} \tag{17}$$

where

$$B = \frac{2c_{11} + C_{33} + 2C_{12} + 4C_{13}}{9} \tag{18}$$

The calculated DFT values of the Young's modulus $E_{<uvw>}$ and Poisson's ratio $\nu_{<uvw>}$ in different crystallographic directions <uvw> of the $P6_3/m$ HA unit cell are given in Table 2.

| Cristallographic direction | Young's modulus, GPa | Poisson's ratio |
|---|---|---|
| <102> | 96 | 0.313 |
| <103> | 94 | 0.315 |
| <311> | 96 | 0.313 |
| <002> | 93 | 0.319 |
| <211> | 98 | 0.309 |
| <202> | 98 | 0.309 |
| <210> | 96 | 0.313 |

Table 2. Young's modulus and Poisson's ratio in different crystallographic directions of a $P6_3/m$ HA unit cell.

The values of $E_{<211>}$ = 98 GPa and $\nu_{<211>}$ = 0.309 were further used for a more precise estimation of the residual stresses in plasma-sprayed double-layer coatings with $TiO_2$ transition and top HA layers (Gueorguiev et al., 2009a).

## 3. Conclusion

Despite the recent advances in research on structural parameters of plasma-sprayed bioceramic coatings and their influence on the operational properties, fundamental knowledge in this field is still insufficient. Non-destructive methods, focused on investigation and control of crystallographic structure and mechanical properties of such coatings are described and adopted. In addition, the complex approach for fundamental and applicable interdisciplinary analyses contributes to better understanding of the structure

formation processes from a physical point of view and has a positive impact on the practical applications of plasma-sprayed bioceramic coatings.

## 4. Acknowledgment

Prof. R. Geoff Richards, director of the AO Research Institute Davos for fruitful discussions and expert opinions.

National Science Fund grants VU-F-205/2006, DO-02-136/2008 and DO-02-167/2008 for calculation time on PHYSON computer cluster.

## 5. References

Azarmi, F.; Coyle, T. & Mostaghimi, J. (2008). Optimization of Atmospheric Plasma Spray Process Parameters using a Design of Experiment for Alloy 625 coatings. *Journal of Thermal Spray Technology,* Vol.17, No.1, (March 2008), pp. 144-155, ISSN 1059-9630

Brossa, F. & Lang, E. (1992). Plasma Spraying – a Versatile Coating Technique, In: *Mechanical and Materials Science: Advanced Techniques for Surface Engineering*, Gissler, W. & Jehn, H. (Eds.), pp. 199-252, ISBN 0-7923-2006-9, Kluwer Academic Publishers, London, UK

Boulos, M.; Fauchais, P.; Vandelle, A. & Pfender, E. (1993). Fundamentals of Plasma Particle Momentum and Heat Transfer, In: *Plasma Spraying: Theory and Applications*, Suryanarayanan, R. (Ed.), pp. 3-60, ISBN 981-02-1363-8, World Scientific, New Jersey, USA

Burgess, A.; Story, B.; La, D.; Wagner, W & LeGeros, J. (1999). Highly Crystalline MP-1 Hydroxylapatite Coating Part I: In Vitro Characterization and Comparison to Other Plasma-Sprayed Hydroxylapatite Coatings. *Clinical Oral Implants Research,* Vol.10, No.4, (August 1999), pp. 245-256, ISSN 1600-0501

Celik, E.; Demirkiran, A. & Avci, E. (1999). Effect of Grit Blasting of Substrate on the Corrosion Behaviour of Plasma-Sprayed $Al_2O_3$ Coatings. *Surface and Coatings Technology,* Vol.116-119, No.1, (September 1999), pp. 1061-1064, ISSN 0257-8972

Chen, S.; Siitonen, P. & Kettunen, P. (1993). Experimental Design and Optimization of Plasma Sprayed Coatings, In: *Plasma Spraying: Theory and Applications*, Suryanarayanan, R. (Ed.), pp. 95-120, ISBN 981-02-1363-8, World Scientific, New Jersey, USA

Choi, H.; Kang, B.; Choi, W.; Choi, D., Choi, S.; Kim, J.; Park, Y & Kim, G. (1998). Effect of the Thickness of Plasma-Sprayed Coating on Bond Strength and Thermal Fatigue Characteristics. *Journal of Materials Science,* Vol.33, No.24, (December 1998), pp. 5895-5899, ISSN 0022-2461

Chou, B. & Chang, E. (2002). Plasma-Sprayed Hydroxyapatite Coating on Titanium Alloy with $ZrO_2$ Second Phase and $ZrO_2$ Intermediate Layer. *Surface and Coatings Technology,* Vol.153, No.1, (April 2002), pp. 84-92, ISSN 0257-8972

Clyne, T. & Gill, S. (1996). Residual Stresses in Thermal Spray Coatings and Their Effect on Interfacial Adhesion: A Review of Recent Work. *Journal of Thermal Spray Technology,* Vol.5, No.4, (December 1996), pp. 401-418, ISSN 1059-9630

Cofino, B.; Fogarassy, P.; Millet, P. & Lodini, A. (2004). Thermal Residual Stresses near the Interface between Plasma Sprayed Hydroxyapatite and Titanium Subtrate. *Journal of Biomedical Materials Research Part A,* Vol.70A, No.1, (July 2004), pp. 20-27, ISSN 1549-3296

Dhiman, R. & Chandra, S. (2007). Predicting Splat Morphology in a Thermal Spray Process, In: *Thermal Spray 2007: Global Coating Solutions,* Marple, B.; Hyland, M.; Lau, Y.; Lima, R. & Montavon, G. (Eds.), pp. 207-212, ASM International, Materials Park, Ohio, USA

Ding, S.; Su, Y.; Ju, C. & Lin, J. (2001). Structure and Immersion Behavior of Plasma-Sprayed Apatite-Matrix Coatings. *Biomaterials,* Vol.22, No.8, (April 2001), pp. 833-845, ISSN 0142-9612

Duan, K. & Wang, R. (2006). Surface Modifications of Bone Implants through Wet Chemistry. *Journal of Materials Chemistry,* Vol.6, No.24, (April 2006), pp. 2309-2322, ISSN 0959-9428

Dyshlovenko, S.; Pawlowski, L. & Roussel, P. (2005). Experimental Investigation of Influence of Plasma Spraying Operational Parameters on Properties of Hydroxyapatite, *Proceedings of the International Thermal Spray Conference,* pp. 726-731, Basel, Switzerland, May 2-4, 2005

Fan, Q.; Wang, L.; Wang, F. & Wang, Q. (2005). Modeling of Temperature and Residual Stress Fields Resulting from Impacting Process of a Molten Ni Particle onto a Flat Substrate, *Proceedings of the International Thermal Spray Conference,* pp. 275-279, Basel, Switzerland, May 2-4, 2005

Frayssinet, P.; Hardy, D. & Rouquet, N. (2006). The Role of Hydroxylapatite Coating Characteristics in Bone Integration after Two Decades of Follow-up in Human Beings, *Proceedings of the International Thermal Spray Conference,* pp. 35-40, Seattle, Washington, USA, May 15-18, 2006

Gaona, M.; Lima, R. & Marple, B. (2007). Nanostructured Titania/Hydroxyapatite Composite Coatings Deposited by High Velocity Oxy-Fuel (HVOF) Spraying. *Materials Science and Engineering: A,* Vol.458, No.1-2, (June 2007), pp. 141-149, ISSN 0921-5093

Gergov,B.; Iordanova, I. & Velinov, T. (1990). A Complex Investigation of Structure and Properties of Thermally Sprayed Ni and Cu-Based Coatings. *Revue de Physique Appliquee,* Vol.20, No.12, (December 1990), pp. 1197-1204, ISSN 0302-0738

Giannozzi, P.; Baroni, S.; Bonini, N.; Calandra, M.; Car, R.; Cavazzoni, C.; Ceresoli, D.; Chiarotti, G. L.; Cococcioni, M.; Dabo, I.; Dal Corso, A.; Fabris, S.; Fratesi, G.; de Gironcoli, S.; Gebauer, R.; Gerstmann, U.; Gougoussis, C.; Kokalj, A.; Lazzeri, M.; Martin-Samos, L.; Marzari, N.; Mauri, F.; Mazzarello, R.; Paolini, S.; Pasquarello, A.; Paulatto, L.; Sbraccia, C.; Scandolo, S.; Sclauzero, G.; Seitsonen, A. P.; Smogunov A.; Umari, P. & Wentzcovitch, R. M. (2009). Quantum Espresso: a Modular and Open-Source Software Project for Quantum Simulations of Materials. *Journal of Physics: Condensed Matter*, Vol.21, No.39, (September 2009), pp. 395502-395521, ISSN 0953-8984

Gill, B. & Tucker, R. (1986). Plasma Spray Coating Processes. *Journal of Materials Science and Technology,* Vol.2, No.1, (January 1986), pp. 207-213, ISSN 1005-0302

Gonze, X. (1996). Towards a Potential-Based Conjugate Gradient Algorithm for Order-N Self-Consistent Total Energy Calculations. *Physical Review B: Condensed Matter and Materials Physics,* Vol.54, No.7, (August 1996), pp. 4383-4386, ISSN 0163-1829

Gueorguiev, B.; Iordanova, I. & Sprecher, C. (2008). Crystallography of Hydroxylapatite Films Applied by Flame Spraying on TAV Substrates, *Proceedings of the 15th Workshop on Plasmatechnik*, pp. 25-32, Ilmenau, Germany, June 26-27, 2008

Gueorguiev, B.; Iordanova, I. & Sprecher, C. (2008). Evaluation of Spherical Grains in Flame-Sprayed Coatings for Medical Purposes by Stereological Methods. *Bulgarian Journal of Physics,* Vol.35, No.2, (December 2008), pp. 119-128, ISSN 1310-0157

Gueorguiev, B.; Iordanova, I.; Sprecher, C. & Skulev, H. (2008). Surface Engineered Titanium Alloys by Application of Bioceramic Coatings for Medical Purposes. *Galvanotechnik,* Vol.99, No.12, (December 2008), pp. 3070-3076, ISSN 0016-4232

Gueorguiev, B.; Sprecher, C.; Antonov, V.; Iordanova, I. & Skulev, H. (2009). Investigation of $TiO_2$ and HA plasma-Sprayed Biomedical Coatings by Structural and DFT Methods, *Proceedings of the 16th Workshop on Plasmatechnik*, pp. 20-26, Ilmenau, Germany, June 25-26, 2009

Gueorguiev, B.; Iordanova, I.; Sprecher, C.; Skulev, H.; Wahl, D. & Hristov, A. (2009). Plasma-Spraying Methods for Applications in the Production of Quality Biomaterials for Modern Medicine and Dentistry. *Journal of Optoelectronics and Advanced Materials,* Vol.11, No.1, (September 2009), pp. 1331-1334, ISSN 1454-4164

Harsha, S.; Dwivedi, D. & Agarwal, A. (2008). Performance of Flame Sprayed Ni-WC Coating under Abrasive Wear Conditions. *Journal of Materials Engineering and Performance,* Vol.17, No.1, (February 2008), pp. 104-110, ISSN 1059-9495

Heimann, R. (2002). Materials Science of Crystalline Bioceramics: a Review of Basic Properties and Applications. *Chiang Mai University Journal of Natural Sciences,* Vol.1, No.1, (January 2002), pp. 23-46, ISSN 16851994

Heimann, R.; Schürmann, N. & Müller, R. (2004). In Vitro and In Vivo Performance of Ti6Al4V Implants with Plasma-Sprayed Osteoconductive Hydroxylapatite–Bioinert Titania Bond Coat "Duplex" Systems: an Experimental Study in Sheep. *Journal of Materials Science: Materials in Medicine,* Vol.15, No.9, (September 2004), pp. 1045-1052, ISSN 0957-4530

Hemmati, I.; Hosseini, H. & Kianvash, A. (2006). The Correlations between Processing Parameters and Magnetic Properties of an Iron–Resin Soft Magnetic Composite. *Journal of Magnetism and Magnetic Materials,* Vol.305, No.1, (October 2006), pp. 147-151, ISSN 0304-8853

Herrmann, M.; Engel, W. & Göbel, H. (2002). Micro Strain in HMX Investigated with Powder X-Ray Diffraction and Correlation with the Mechanical Sensitivity, *Proceedings of the 51th Annual Denver X-Ray Conference Advances in X-Ray Analysis. JCPDS-International Centre for Diffraction Data, Advances in X-Ray Analysis,* Vol.45, No.1, (2002), pp. 212-217, Colorado Springs, Colorado, USA, July 29- August 2, 2002

Iordanova, I. & Forcey, K. (1991). Investigation by Rutherford Back-Scattering Spectrometry of Tin Coatings Electrolytically Applied on Steel Strip. *Materials Science and Technology,* Vol.7, No.1, (January 1991), pp. 20-23, ISSN 0267-0836

Iordanova, I.; Forcey, K.; Valtcheva, J. & Gergov, B. (1994). An X-ray Study of Thermally-Sprayed Metal Coatings. *Materials Science Forum,* Vol.166-169, No.1, (June 1994), pp. 319-324, ISSN 0255-5476

Iordanova, I.; Forcey, K.; Gergov, B. & Bojinov, V. (1995). Characterization of Flame-Sprayed and Plasma-Sprayed Pure Metallic and Alloyed Coatings. *Surface and Coatings Technology,* Vol.72, No.1-2, (May 1995), pp. 23-29, ISSN 0257-8972

Iordanova, I. & Forcey, K. (1997). Texture and Residual Stresses in Thermally Sprayed Coatings. *Surface and Coatings Technology,* Vol.91, No.3, (May 1997), pp. 174-182, ISSN 0257-8972

Iordanova, I.; Surtchev, M. & Forcey, K. (2001). Metallographic and SEM Investigation of the Microstructure of Thermally Sprayed Coatings on Steel Substrates. *Surface and Coatings Technology,* Vol.139, No.2-3, (May 2001), pp. 118-126, ISSN 0257-8972

Iordanova, I.; Antonov, V. & Gurkovsky, S. (2002). Changes of Microstructure and Mechanical Properties of Cold-Rolled Low Carbon Steel Due to Its Surface Treatment by Nd:Glass Pulsed Laser. *Surface and Coatings Technology,* Vol.153, No.2-3, (April 2002), pp. 174-182, ISSN 0257-8972

Keller, N.; Bertrand, G.; Coddet, C. & Meunier, C. (2003). Influence of Plasma Spray Parameters on Microstructural Characteristics of $TiO_2$ Deposits, In: *Thermal Spray*

*2003: Advancing the Science & Applying the Technology,* Moreau, C. & Marple, B. (Eds.), pp. 1403-1408, ASM International, Materials Park, Ohio, USA

Khor, K.; Gu, Y.; Pan, D. & Cheang, P. (2004). Microstructure and Mechanical Properties of Plasma Sprayed HA/YSZ/Ti–6Al–4V Composite Coatings. *Biomaterials,* Vol.25, No.18, (August 2004), pp. 4009-4017, ISSN 0142-9612

Kreye, H.; Schwetzke, R. & Zimmermann, S. (2007). High Velocity Oxy-Fuel Flame Spraying Process and Coating Characteristics, In: *Thermal Spray 1996: Practical Solutions for Engineering Problems,* Berndt, C. (Ed.), pp. 451-456, ASM International, Materials Park, Ohio, USA

Kuroda, S. & Clyne, T. (1991). The Quenching Stress in Thermally Sprayed Coatings. *Thin Solid Films,* Vol.200, No.1, (May 1991), pp. 49-66, ISSN 0040-6090

LeGeros, W. (2002). Properties of Osteoconductive Biomaterials: Calcium Phosphates. *Clinical Orthopaedics and Related Research,* Vol.395, No.1, (February 2001), pp. 81-95, ISSN 1528-1132

Leigh, S. & Berndt, C. (1997). Evaluation of Off-Angle Thermal Spray. *Surface and Coatings Technology,* Vol.89, No.3, (March 1997), pp. 213-224, ISSN 0257-8972

Li, C. & Ohmori, A. (2002). Relationships between the Microstructure and Properties of Thermally Sprayed Deposits. *Journal of Thermal Spray Technology,* Vol.11, No.3, (September 2002), pp. 365-374, ISSN 1059-9630

Li, H.; Khor, K. & Cheang, P. (2004). Thermal Sprayed Hydroxyapatite Splats: Nanostructures, Pore Formation Mechanisms and TEM Characterization. *Biomaterials,* Vol.25, No.17, (August 2004), pp. 3463-3471, ISSN 0142-9612

Li, Y. & Khor, K. (2002). Microstructure and Composition Analysis in Plasma Sprayed Coatings of $Al_2O_3/ZrSiO_4$ Mixtures. *Surface and Coatings Technology,* Vol.150, No.2-3, (February 2002), pp. 125-132, ISSN 0257-8972

Liu, F.; Zeng, K.; Wang, H.; Zhao, X.; Ren,X. & Yu, Y. (2005). Numerical Investigation on the Heat Insulation Behaviour of Thermal Spray Coating by Unit Cell Model, *Proceedings of the International Thermal Spray Conference*, pp. 806-810, Maastricht, Netherlans, June 2-4, 2008

Liu, X.; Zhao, X. & Ding, C. (2006). Introduction of Bioactivity to Plasma Sprayed $TiO_2$ Coating with Nanostructured Surface by Post-Treatment, *Proceedings of the International Thermal Spray Conference,* pp. 53-57, Seattle, Washington, USA, May 15-18, 2006

Lugscheiber, E.; Oberländer, B. & Rouhaghdam, A. (1993). Optimising the APS-Process Parameters for New Ni-Hardfacing Alloys Using a Mathematical Model, In: *Plasma Spraying: Theory and Applications*, Suryanarayanan, R. (Ed.), pp. 141-162, ISBN 981-02-1363-8, World Scientific, New Jersey, USA

Mawdsley, J.; Su, Y.; Faber, K. & Bernecki, T. (2001). Optimization of Small-Particle Plasma-Sprayed Alumina Coatings Using Designed Experiments. *Materials Science and Engineering: A,* Vol.308, No.1-2, (June 2001), pp. 189-199, ISSN 0921-5093

McPherson, R.; Gane, N. & Bastow, J. (1995). Structural haracterization of Plasma-Sprayed Hydroxylapatite Coatings. *Journal of Materials Science: Materials in Medicine,* Vol.6, No.6, (June 1995), pp. 327-334, ISSN 0957-4530

Monkhorst, H. & Pack, J. (1976). Special Points for Brillouin-Zone Integrations. *Physical Review B: Condensed Matter and Materials Physics,* Vol.13, No.12, (June 1976), pp. 5188-5192, ISSN 0163-1829

Montavon, A.; Sampath, S.; Berndt, C.; Herman, H. & Coddet, C. (1997). Effects of the Spray Angle on Splat Morphology During Thermal Spraying. *Surface and Coatings Technology,* Vol.91, No.1-2, (May 1997), pp. 107-115, ISSN 0257-8972

Moreau, C.; Bisson, J.; Lima, R. & Marple, B. (2005). Diagnostics for Advanced Materials Processing by Plasma Spraying. *Pure and Applied Chemistry,* Vol.77, No.2, (February 2005), pp. 443-462, ISSN 0033-4545

Morris, H. & Ochi, K. (1998). Hydroxyapatite-Coated Implants: a Case for Their Use. *Journal of Oral and Maxillofacial Surgery,* Vol.56, No.11, (November 1998), pp. 1303-1311, ISSN 0278-2391

Nelea, V.; Mihailescu, I. & Jelinek, M. (2007). Biomaterials: New Issues and Breakthroughs for Biomedical Applications, In: *Pulsed Laser Deposition of Thin Films: Applications-Led Growth of Functional Materials*, Eason, R. (Ed.), pp. 421-459, John Wiley & Sons, Inc., London, UK

Neufuss, K.; Ilavsky, J.; Kolman, B.; Dubsky, J.; Rohan, P. & Chraska, P. (2001). Variation of Plasma Spray Deposits Microstructure and Properties Formed by Particles Passing through Different Areas of Plasma Jet. *Ceramics-Silikaty,* Vol.45, No.1, (March 2001), pp. 1-8, ISSN 0862-5468

Nicoll, A.; Gruner, H.; Prince, R. & Wuest, G. (1985). Thermal Spray Coatings for High Temperature Protection. *Surface Engineering,* Vol.1, No.1, (February 1985), pp. 59-71, ISSN 0267-0844

Ohmori, A. & Li, C. (1991). Quantitative Characterization of the Structure of Plasma-Sprayed $Al_2O_3$ Coating by Using Copper Electroplating. *Thin Solid Films,* Vol.201, No.2, (June 1991), pp. 241-252, ISSN 0040-6090

Parizi, H.; Rosenzweig, L.; Mostaghimi, J.; Chandra, S.; Coyle, T.; Salimi, L.; Pershin, L.; McDonald, A. & Moreau, C. (2007). Numerical Simulation of Droplet Impact on Patterned Surfaces, In: *Thermal Spray 2007: Global Coating Solutions,* Marple, B.; Hyland, M.; Lau, Y.; Lima, R. & Montavon, G. (Eds.), pp. 213-218, ASM International, Materials Park, Ohio, USA

Prevey, P. (1986). X-Ray Diffraction Residual Stress Techniques, In: *Metals Handbook Volume 10: Materials Characterization*, Mills, K.; Davis, J.; Destefani, J. & Dietrich, D. (Eds.), pp. 380-392, ISBN 981-02-1363-8, ASM International, Materials Park, Ohio, USA

Salman, S.; Cal, B.; Gunduz, O.; Agathopoulos, S. & Oktar, F. (2008). The Influence of Bond-Coating on Plasma Sprayed Alumina-Titania, Doped with Biologically Derived Hydroxyapatite, on Stainless Steel, In: *Virtual and Rapid Manufacturing,* Bartolo, P. (Ed.), pp. 289-292, ISBN 978-0-415-41602-3, Taylor & Francis Group, London, UK

Sampath, S.; Jiang, X.; Kulkarni, A.; Matejicek, J.; Gilmore, D. & Neiser, R. (2003). Development of Process Maps for Plasma Spray: Case Study for Molybdenum. *Materials Science and Engineering: A,* Vol.348, No.1-2, (May 2003), pp. 54-66, ISSN 0921-5093

Sarikaya, O. (2005). Effect of Some Parameters on Microstructure and Hardness of Alumina Coatings Prepared by the Air Plasma Spraying Process. *Surface and Coatings Technology,* Vol.190, No.2-3, (January 2005), pp. 388-393, ISSN 0257-8972

Schlegel, H. (1982). Optimization of Equilibrium Geometries and Transition Structures, Vol.3, No.2, (July 1982), pp. 214-218, ISSN 1096-987X

Sirotin, Y. & Shaskolskaya, M. (1983). *Fundamentals of Crystal Physics*, ISBN 978-082-8524-64-3, Imported Publications, New York, USA

Skulev, H.; Malinov, S.; Sha, W. & Basheer, P. (2005). Microstructural and Mechanical Properties of Nickel-Base Plasma Sprayed Coatings on Steel and Cast Iron Substrates. *Surface and Coatings Technology,* Vol.197, No.2-3, (July 2005), pp. 177-184, ISSN 0257-8972

Soares, P.; Mikowski, A.; Lepienski, C.; Santos, E.; Soares, G.; Filho, V. & Kuromoto, N. (2008). Hardness and Elastic Modulus of $TiO_2$ Anodic Films Measured by Instrumented Indentation. *Journal of Biomedical Materials Research Part B: Applied Biomaterials,* Vol.84B, No.2, (February 2008), pp. 524-530, ISSN 1552-4973

Srinivasan, V.; Sampath, S.; Vaidya, A.; Streibl, T. & Friis, M. (2006). On the Reproducibility of Air Plasma Spray Process and Control of Particle State. *Journal of Thermal Spray Technology,* Vol.15, No.4, (December 2006), pp. 739-743, ISSN 1059-9630

Staia, M.; Valente, T.; Bartuli, C.; Lewis, D.; Constable, C.; Roman, A.; Lesage, J.; Chicot, D. & Mesmacque, G. (2001). Part II: Tribological Performance of $Cr_3C_2$-25% NiCr Reactive Plasma Sprayed Coatings Deposited at Different Pressures. *Surface and Coatings Technology,* Vol.146-147, No.1, (September-October 2001), pp. 563-570, ISSN 0257-8972

Streibl, T.; Vaidya, A.; Friis, M.; Srinivasan, V. & Sampath, S. (2006). A Critical Assessment of Particle Temperature Distributions During Plasma Spraying: Experimental Results for YSZ. *Plasma Chemistry and Plasma Processing,* Vol.26, No.1, (February 2006), pp. 73-102, ISSN 0272-4324

Suchanek, W. & Yoshimura, M. (1998). Processing and Properties of Hydroxyapatite-Based Biomaterials for Use as Hard Tissue Replacement Implants. *Journal of Materials Research,* Vol.13, No.1, (January 1998), pp. 94-117, ISSN 0884-2914

Sun, L.; Berndt, C.; Khor, K.; Cheang, H. & Gross, K. (2002). Surface Characteristics and Dissolution Behavior of Plasma-Sprayed Hydroxyapatite Coating. *Journal of Biomedical Materials Research Part A,* Vol.62A, No.2, (November 2002), pp. 228-236, ISSN 1549-3296

Thomas, K. (1994). Hydroxyapatite Coatings. *Orthopedics,* Vol.17, No.3, (March 1994), pp. 267-278, ISSN 0147-7447

Toma, L.; Keller, N.; Bertrand, G.; Klein, D. & Coddet, C. (2003). Elaboration and Characterization of Environmental Properties of $TiO_2$ Plasma Sprayed Coatings. *International Journal of Photoenergy,* Vol.5, No.3, (March 2003), pp. 141-151, ISSN 1110-662X

Tong, W.; Chen, J.; Li, X.; Cao, Y.; Yang, Z.; Feng, J. & Zhang, X. (1996). Effect of Particle Size on Molten States of Starting Powder and Degradation of the Relevant Plasma-Sprayed Hydroxyapatite Coatings. *Biomaterials,* Vol.17, No.15, (August 1996), pp. 1507-1513, ISSN 0142-9612

Tsui, Y.; Doyle, C. & Clyne, T. (1998). Plasma Sprayed Hydroxyapatite Coatings on Titanium Substrates Part 1: Mechanical Properties and Residual Stress Levels. *Biomaterials,* Vol.19, No.22, (November 1998), pp. 2015-2029, ISSN 0142-9612

Wallace, J. & Ilavsky, J. (1998). Elastic Modulus Measurements in Plasma Sprayed Deposits. *Journal of Thermal Spray Technology,* Vol.7, No.4, (December 1998), pp. 521-526, ISSN 1059-9630

Yu-Peng, L.; Mu-Sen, L.; Shi-Tong, L.; Zhi-Gang, W. & Rui-Fu, Z. (2004). Plasma-Sprayed Hydroxyapatite+Titania Composite Bond Coat for Hydroxyapatite Coating on Titanium Substrate. *Biomaterials,* Vol.25, No.18, (August 2004), pp. 4393-4403, ISSN 0142-9612

Zhao, X.; Chen, Z.; Liu, X. & Ding, C. (2007). Preparation, Microstructure and Bioactivity of Plasma-Sprayed $TiO_2$ Coating, In: *Thermal Spray 2007: Global Coating Solutions,* Marple, B.; Hyland, M.; Lau, Y.; Lima, R. & Montavon, G. (Eds.), pp. 397-400, ASM International, Materials Park, Ohio, USA

Zhu, S. & Ding, C. (2000). Characterization of Plasma Sprayed Nano-Titania Coatings by Impedance Spectroscopy. *Journal of the European Ceramic Society,* Vol.20, No.2, (February 2000), pp. 127-131, ISSN 0955-2219

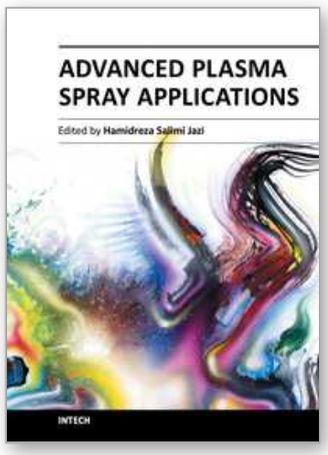


**Advanced Plasma Spray Applications**
Edited by Dr. Hamid Jazi

ISBN 978-953-51-0349-3
Hard cover, 250 pages
**Publisher** InTech
**Published online** 21, March, 2012
**Published in print edition** March, 2012

Recently, plasma spray has been received a large number of attentions for various type of applications due to the nature of the plasma plume and deposition structure. The plasma gas generated by the arc, consists of free electrons, ionized atoms, some neutral atoms, and undissociated diatomic molecules. The temperature of the core of the plasma jet may exceed up to 30,000 K. Gas velocity in the plasma spray torch can be varied from subsonic to supersonic using converging-diverging nozzles. Heat transfer in the plasma jet is primarily the result of the recombination of the ions and re-association of atoms in diatomic gases on the powder surfaces and absorption of radiation. Taking advantages of the plasma plume atmosphere, plasma spray can be used for surface modification and treatment, especially for activation of polymer surfaces. I addition, plasma spray can be used to deposit nanostructures as well as advanced coating structures for new applications in wear and corrosion resistance. Some state-of-the-art studies of advanced applications of plasma spraying such as nanostructure coatings, surface modifications, biomaterial deposition, and anti wear and corrosion coatings are presented in this book.

**How to reference**
In order to correctly reference this scholarly work, feel free to copy and paste the following:

Ivanka Iordanova, Vladislav Antonov, Christoph M. Sprecher, Hristo K. Skulev and Boyko Gueorguiev (2012). Plasma Sprayed Bioceramic Coatings on Ti-Based Substrates: Methods for Investigation of Their Crystallographic Structures and Mechanical Properties, Advanced Plasma Spray Applications, Dr. Hamid Jazi (Ed.), ISBN: 978-953-51-0349-3, InTech, Available from: http://www.intechopen.com/books/advanced-plasma-spray-applications/plasma-sprayed-bioceramic-coatings-on-ti-based-substrates-methods-for-investigation-of-their-crystal

INTECH
open science | open minds

**InTech Europe**
University Campus STeP Ri
Slavka Krautzeka 83/A
51000 Rijeka, Croatia
Phone: +385 (51) 770 447
Fax: +385 (51) 686 166
www.intechopen.com

**InTech China**
Unit 405, Office Block, Hotel Equatorial Shanghai
No.65, Yan An Road (West), Shanghai, 200040, China
中国上海市延安西路65号上海国际贵都大饭店办公楼405单元
Phone: +86-21-62489820
Fax: +86-21-62489821

IntechOpen